

Electronic Supplementary Information

A multi-ratiometric fluorescence sensor integrated intrinsic signal amplification strategy for sensitive and visual assay of anthrax biomarker based on bimetallic lanthanide metal-organic framework

Lei Han,^{a,b} Xue Zhen Dong,^a Shi Gang Liu,^a Xiao Hu Wang,^a Yu Ling,^a Nian Bing Li,^{*a} and Hong Qun Luo ^{*a}

^a Key Laboratory of Luminescence Analysis and Molecular Sensing, School of Chemistry and Chemical Engineering, Southwest University, Chongqing 400715, P. R. China

^b Faculty of Science, Kunming University of Science and Technology, Kunming 650500, Yunnan, P. R. China

*Corresponding Authors

* Nian Bing Li and Hong Qun Luo

* No.2 Tiansheng Road Beibei District, Chongqing 400715, P. R. China.

E-mail address: linb@swu.edu.cn, luohq@swu.edu.cn

Table of Contents

Instruments	S-3
Synthesis of Eu-MOF and Tb-MOF	S-4
Bacterial spore study	S-4
Paper-based sensing of DPA	S-5
Fig. S1 The pore size distribution of Tb/Eu-MOF	S-6
Table S1. The atomic percent of Tb/Eu-MOF by EDS analysis	S-6
Fig. S2 PXRD patterns of the Tb/Eu-MOF under different conditions	S-7
Fig. S3 Fluorescence spectra of Tb/Eu-MOF under different conditions	S-7
Fig. S4 The TGA curve of Tb/Eu-MOF	S-8
Fig. S5 Optimization of the excitation wavelength for DPA detection	S-8
Fig. S6 Optimization of pH of the sensing system	S-9
Fig. S7 Optimization of the incubation time for DPA detection	S-9
Table S2. Comparison of some reported methods for DPA detection	S-10
Fig. S8 Paper-based sensing of DPA	S-11
Table S3. Detection results of DPA in lake water samples	S-12
References	S-13

Instruments. Scanning electron microscopy (SEM) measurements were performed on a ZEISS MERLIN Compact scanning electron microscope (ZEISS, Germany). Powder X-ray diffraction (PXRD) patterns were collected from a Bruker D2 Phaser X-ray diffractometer (Bruker, Germany) with Cu K α radiation over the 2θ range from 5 to 60°. Fluorescence spectra were collected on a Hitachi F-7100 spectrofluorometer (Hitachi, Japan). The influences from the second-order scattering peaks were eliminated by placing a JB400 filter before the detector. Fluorescence lifetimes were obtained from a Horiba Jobin Yvon Fluorolog-3 spectrofluorometer (Horiba, USA). Transmission electron microscopy (TEM) images were collected by FEI Talos S-FEG transmission electron microscopy (FEI, USA) and scanning transmission electron microscopy (STEM) images were obtained from a high-angle annular dark field (HAADF) detector. UV-vis absorption spectra were carried out at a UV-2450 spectrophotometer (Shimadzu, Japan). X-ray photoelectron spectroscopy (XPS) tests were performed on a Thermo Scientific K-Alpha+ X-ray photoelectron spectrometer (Thermo Scientific, USA). Fourier transform infrared (FT-IR) spectra were collected by using a Bruker IFS 113v spectrometer (Bruker, Germany). Thermogravimetric analysis (TGA) was carried out on a Mettler TGA 2 analyzer (Mettler, Switzerland) from 30 °C to 790 °C with a heating rate of 5 °C min⁻¹ under the flow of N₂. The single-crystal X-ray diffraction measurement was performed on a BRUKER D8 VENTURE PHOTON II area-detector diffractometer with graphite-monochromated Mo-K α radiation ($\lambda = 0.71073 \text{ \AA}$) at 296 K. The N₂ adsorption-desorption isotherm was recorded with an Autosorb IQ surface area and pore analyzer at 77 K under liquid N₂.

Synthesis of Eu-MOF and Tb-MOF. The Eu-MOF was synthesized according to a previous paper with some modifications.¹ Detailedly, a portion of 0.0264 g of H₂BDC-OH (0.145 mmol), 0.0647 mg of Eu(NO₃)₃·6H₂O (0.145 mmol), and 0.1623 g of FBA (1.158 mmol) were added to 7.3 mL of DMF and then vigorously stirred for dissolution. Subsequently, 0.6 mL of H₂O and 0.2 mL of 3.5 M DMF diluted HNO₃ was added to the above solution. After mixing well, the mixture was transferred into a Teflon autoclave and heated at 120°C for 48 h. The other processes are the same as the synthesis process of Tb/Eu-MOF. The synthesis of Tb-MOF was similar to that of Eu-MOF except that Tb(NO₃)₃·5H₂O was used instead of Eu(NO₃)₃·6H₂O.

Bacterial spore study. Bacterial spore cultures were implemented by the previously reported methods with some modification.²⁻⁴ Firstly, the resuscitation solution was added to the freeze-dried *Bacillus subtilis* (CMCC(B)63501) strain to prepare the suspension. Subsequently, a certain amount of *Bacillus subtilis* suspension was inoculated on Luria-Bertani medium (10 g/L tryptone, 5 g/L yeast extract, 10 g/L NaCl), and then incubated at 37 °C for 4 days. After incubation, the samples were washed with sterile ultrapure water 5 times to remove the culture medium. After that, about 3 mg of samples were dispersed into 1 mL of 10 mM D-alanine solution, and the suspension was then heated in a water bath at 70 °C for 90 min to germinate the spores and release DPA. After cooling to room temperature, the above-mentioned solution was filtered with a 0.22 μM membrane filter to remove bacteria.

Paper-based sensing of DPA. For the paper-based sensing of DPA, the test papers were fabricated by immersing nitrocellulose filter paper into the Tb/Eu-MOF solution.

Firstly, the nitrocellulose filter paper was cut into the circular tablet by a hole puncher, and then the circular filter paper was immersed into the Tb/Eu-MOF probe solution. After natural drying of the filter paper loaded with the Tb/Eu-MOF, the test papers were used for subsequent paper-based sensing.

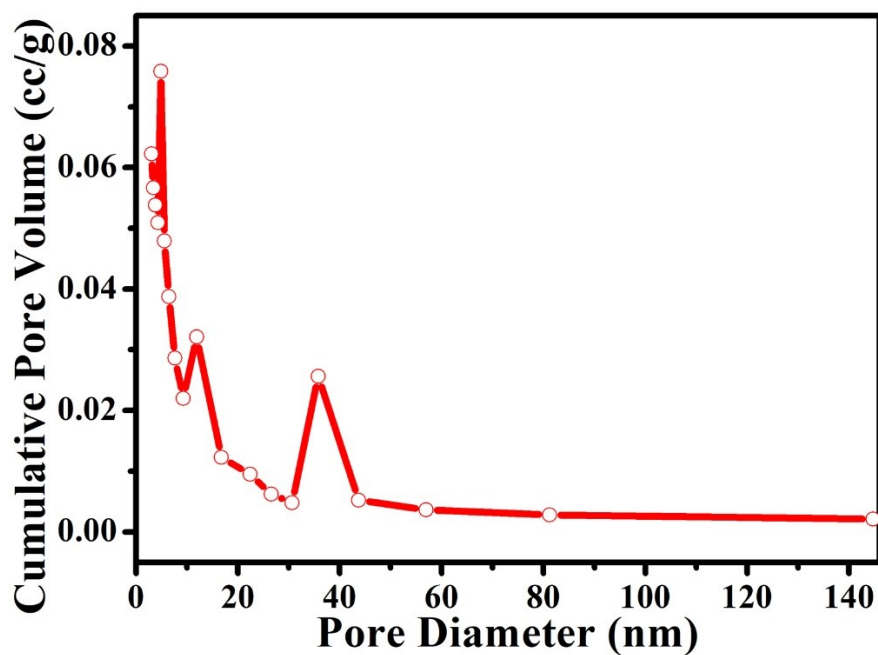


Fig. S1 The pore size distribution of Tb/Eu-MOF calculated from N₂ sorption isotherms by the Barrett-Joyner-Halenda model.

Table S1. The atomic percent of Tb/Eu-MOF by EDS analysis.

Element	Atomic percent (%)
C	75.2
O	17.65
F	5.22
Eu	0.92
Tb	1.01

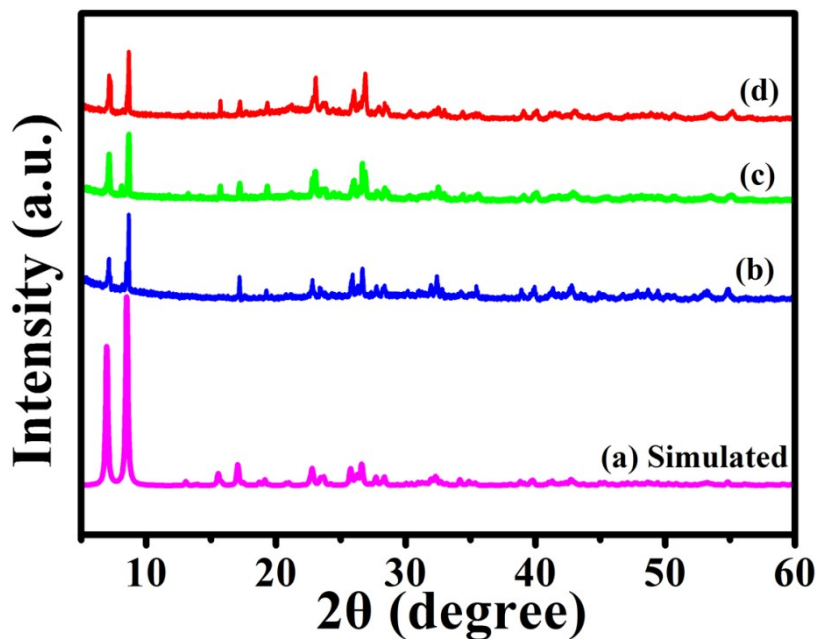


Fig. S2 (a) Simulated XRD and (b) PXRD patterns of the Tb/Eu-MOF. PXRD patterns of the Tb/Eu-MOF after soaked in water for (c) 1 day and (d) 2 days.

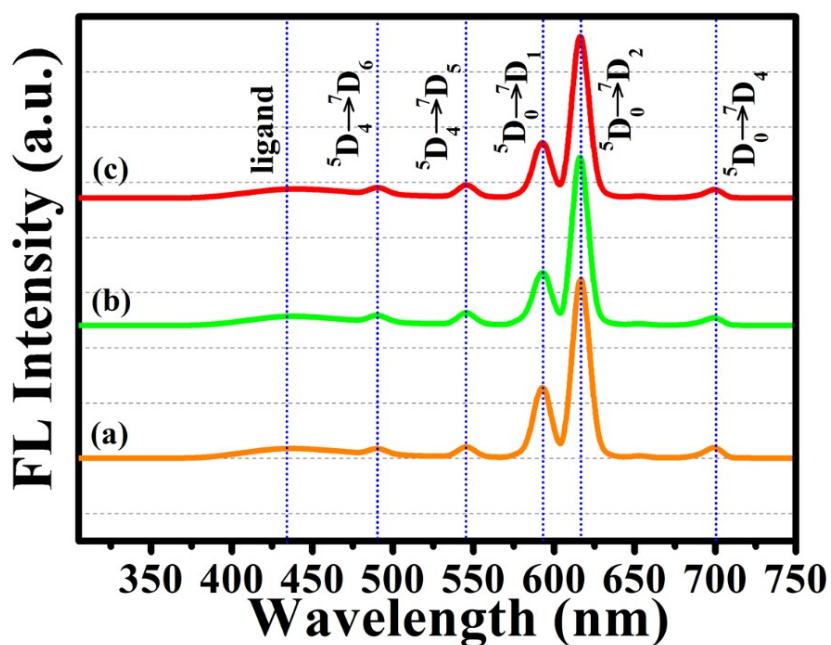


Fig. S3 Fluorescence spectra of solid-state for (a) Tb/Eu-MOF, (b) Tb/Eu-MOF after soaked in water for 1 day, and (c) Tb/Eu-MOF after soaked in water for 2 days.

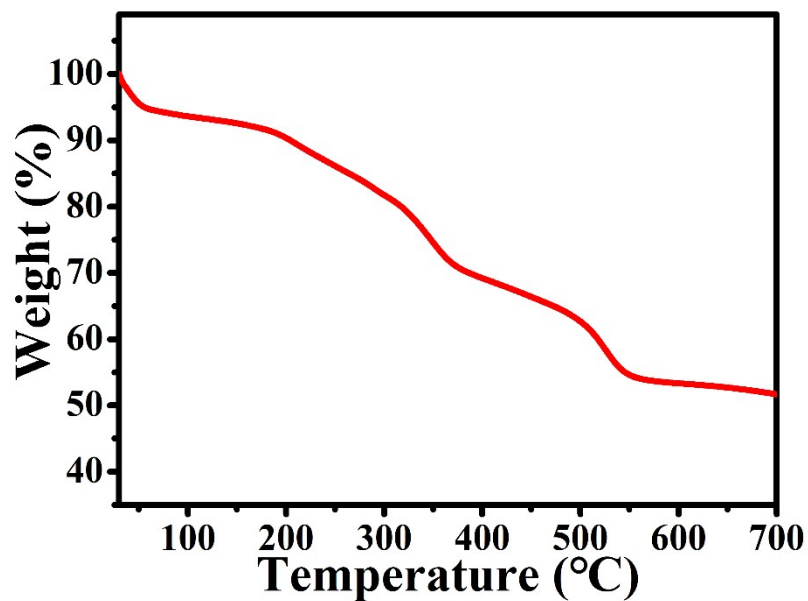


Fig. S4 The TGA curve of Tb/Eu-MOF.

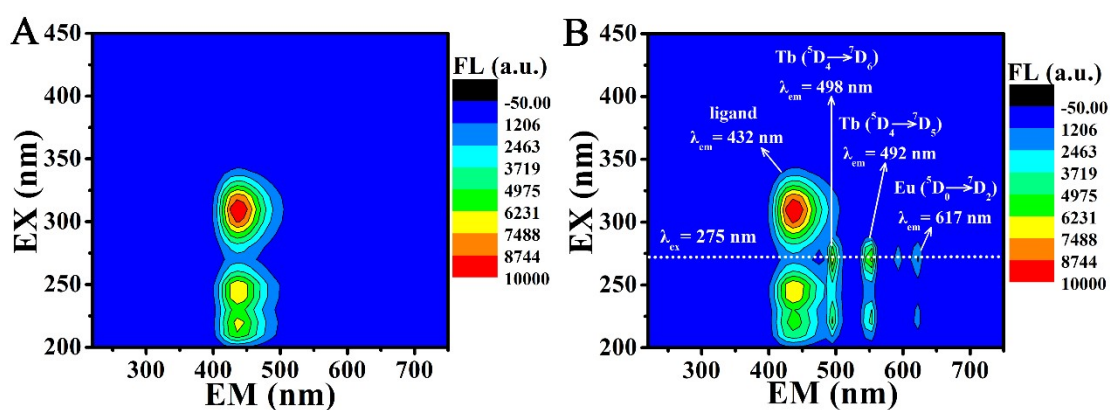


Fig. S5 Optimization of the excitation wavelength for DPA detection: three-dimensional fluorescence spectra of Tb/Eu-MOF (2.5 mg/L) in Tris-HCl buffer (pH 7.5) before (A) and after (B) the addition of 20 μM DPA.

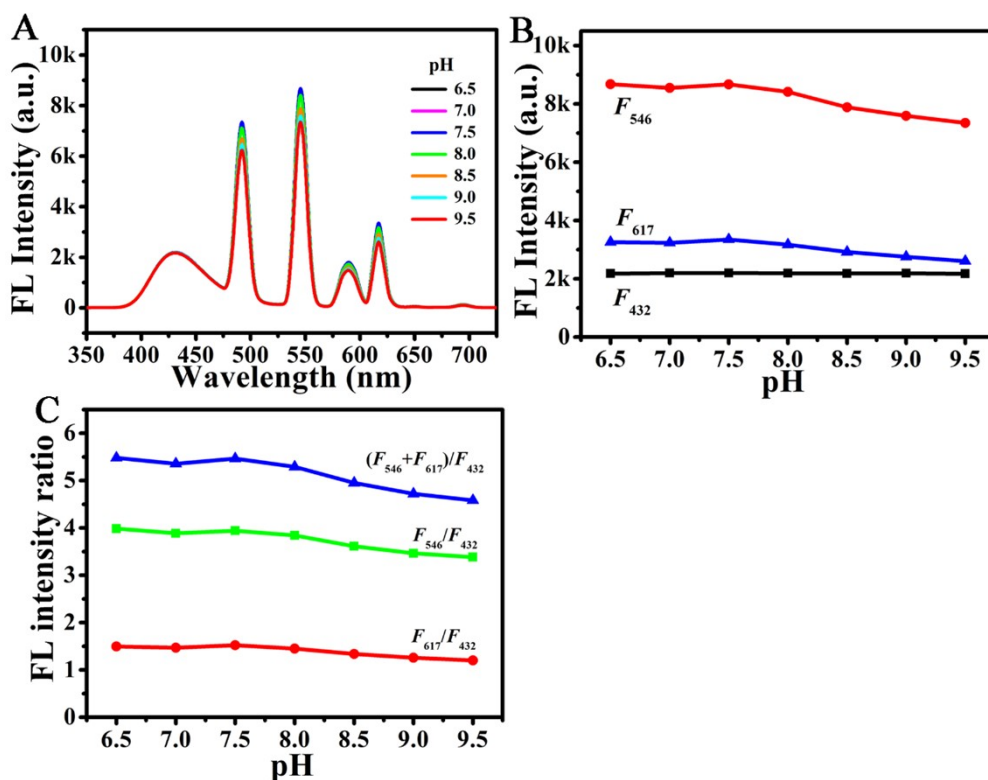


Fig. S6 Optimization of the pH of sensing system: (A) Fluorescence spectra, (B) fluorescence intensity, and (C) fluorescence intensity ratio of Tb/Eu-MOF (2.5 mg/L) in the Tris-HCl buffer (50 mM) at different pH values after the addition of 20 μ M DPA.

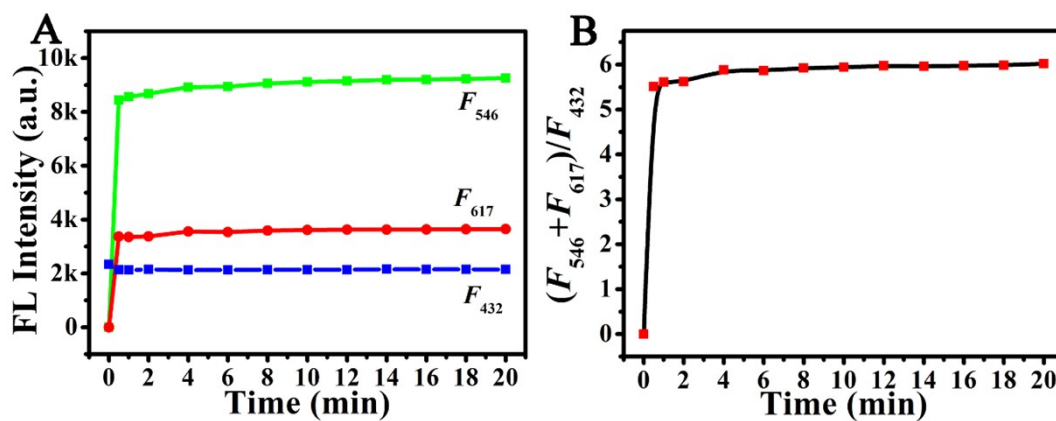


Fig. S7 Optimization of the incubation time for ratiometric fluorescence sensing of DPA. Experimental conditions: Tb/Eu-MOF, 2.5 mg/L; DPA, 20 μ M; 50 mM Tris-HCl buffer, pH 7.5; $\lambda_{\text{ex}} = 275$ nm.

Table S2. Comparison of the reported fluorescence methods for DPA detection.

Probe	Sensing mode	Linear range (μM)	LOD (nM)	Ref.
Eu-MOF	Turn-on	0 – 100	3800	5
^a His@ZIF-8/Tb ³⁺	Turn-on	0.08 – 10	20	6
^b TbP-CPs	Turn-on	0 – 8	5	7
^c Sm ³⁺ /GSH@AuNCs	Turn-off	1 – 120	100	8
^d Ln-CPNs	Ratiometric FL	2 – 16	96	4
^e CDs-Tb	Ratiometric FL	0.005 – 1.2	5	9
^f Eu@SiNPs	Ratiometric FL	0.5 – 20	150	10
^g Tb-Micelle	Ratiometric FL	0 – 7	54	11
^h R6G/CdS@ZIF-8	Ratiometric FL	0.1 – 150	67	12
ⁱ Eu-CDs	Ratiometric FL	0.005 – 0.7	5	13
^j Tb-COP	Ratiometric FL	0.1 – 30	13.5	14
Eu-CDs	Ratiometric FL	0.5 – 110	50	15
Tb/Eu-MOF	Ratiometric FL	0.05 – 20	1.5	This work

^a His@ZIF-8/Tb³⁺: Tb³⁺-doped histidine functionalized ZIF-8; ^b TbP-CPs: terbium phosphonate coordination polymer microspheres; ^c Sm³⁺/GSH@AuNCs: Sm³⁺ induced glutathione-protected gold nanoclusters; ^d Ln-CPNs: lanthanide coordination polymer nanoparticles; ^e CDs-Tb: Tb³⁺ functionalized carbon dots; ^f Eu@SiNPs: Eu³⁺-doped silicon nanoparticles; ^g Tb-Micelle: Tb³⁺ functionalized micelle; ^h R6G/CdS@ZIF-8: rhodamine 6G and CdS quantum dots-loaded ZIF-8; ⁱ Eu-CDs: Eu³⁺-doped carbon dots; ^j Tb-COP: terbium-covalent organic polymer.

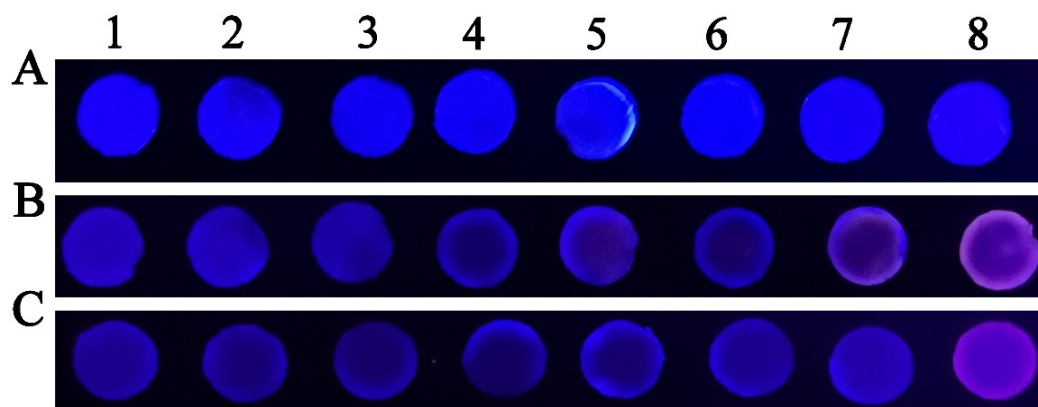


Fig. S8 (A) Photographs of the nitrocellulose filter paper loaded with Tb/Eu-MOF under irradiation at a 275 nm UV lamp. Photographs of the test paper loaded with Tb/Eu-MOF upon addition of (B) 8 μ L of DPA solution with variable concentrations (from 1 to 8: 0, 50 μ M, 100 μ M, 250 μ M, 500 μ M, 750 μ M, 1 mM, and 5 mM) and (C) 8 μ L of 5 mM different interferences (from 1 to 8: H₂O, BA, *p*-HBA, *o*-PA, *m*-PA, BTC, Phe, Asp, and DPA) under irradiation at a 275 nm UV lamp.

Table S3. Detection results of DPA in lake water samples (n = 3).

Sample	Added (μM)	Detection signal	Found (μM)	Recovery (%)	RSD (%)
	0		NF ^a	–	–
	4	F_{546}/F_{423}	4.36	109.0	1.2
	8		8.87	110.9	1.4
	12		12.58	104.8	0.8
	0		NF	–	–
Lake	4	F_{617}/F_{423}	4.87	121.8	0.9
water	8		8.97	112.1	0.4
	12		11.48	95.7	0.3
	0		NF	–	–
	4	$(F_{546}+F_{617})/F_{423}$	4.06	101.5	1.0
	8		7.90	98.8	1.4
	12		11.74	97.8	0.7

^a Not found.

References

1. T. F. Xia, Y. T. Wan, Y. P. Li, J. Zhang, Highly stable lanthanide metal-organic framework as an internal calibrated luminescent sensor for glutamic acid, a neuropathy biomarker, *Inorg. Chem.* 2020, **59**, 8809–8817.
2. C. Y. Huang, R. X. Ma, Y. X. Luo, G. Y. Shi, J. J. Deng, T. S. Zhou, Stimulus response of TPE-TS@Eu/GMP ICPs: toward colorimetric sensing of an anthrax biomarker with double ratiometric fluorescence and its coffee ring test kit for point-of-use application, *Anal Chem* 2020, **92**, 12934–12942.
3. P. R. Su, L. J. Liang, T. Wang, P. P. Zhou, J. Cao, W. S. Liu, Y. Tang, AIE-based Tb³⁺ complex self-assembled nanoprobe for ratiometric fluorescence detection of anthrax spore biomarker in water solution and actual spore samples, *Chem. Eng. J.* 2021, **413**, 127408.
4. N. Gao, Y. F. Zhang, P. C. Huang, Z. H. Xiang, F. Y. Wu, L. Q. Mao, Perturbing tandem energy transfer in luminescent heterobinuclear lanthanide coordination polymer nanoparticles enables real-time monitoring of release of the anthrax biomarker from bacterial spores, *Anal. Chem.* 2018, **90**, 7004–7011.
5. D. Wu, Z. Zhang, X.W. Chen, L.K. Meng, C.G. Li, G.H. Li, X.B. Chen, Z. Shi, S.H. Feng, A non-luminescent Eu-MOF-based "turn-on" sensor towards an anthrax biomarker through single-crystal to single-crystal phase transition, *Chem. Commun.* 2019, **55**, 14918–14921.
6. L. Guo, M. S. Liang, X. L. Wang, R. M. Kong, G. Chen, L. Xia, F. L. Qu, The role of l-histidine as molecular tongs: a strategy of grasping Tb³⁺ using ZIF-8 to design

- sensors for monitoring an anthrax biomarker on-the-spot, *Chem. Sci.* 2020, **11**, 2407–2413.
7. Y. Q. Luo, L. Zhang, L. Y. Zhang, B. H. Yu, Y. J. Wang, W. B. Zhang, Multiporous terbium phosphonate coordination polymer microspheres as fluorescent probes for trace anthrax biomarker detection, *ACS Appl. Mater. Interfaces* **2019**, *11*, 15998–16005.
 8. M. I. Halawa, B. S. Li, G. B. Xu, Novel synthesis of thiolated gold nanoclusters induced by lanthanides for ultrasensitive and luminescent detection of the potential anthrax spores' biomarker, *ACS Appl. Mater. Interfaces* 2020, **12**, 32888–32897.
 9. H. Chen, Y. J. Xie, A. M. Kirillov, L. L. Liu, M. H. Yu, W. S. Liu, Y. Tang, A ratiometric fluorescent nanoprobe based on terbium functionalized carbon dots for highly sensitive detection of an anthrax biomarker, *Chem. Commun.* 2015, **51**, 5036–5039.
 10. M. Na, S. P. Zhang, J. J. Liu, S. D. Ma, Y. X. Han, Y. Wang, Y. X. He, H. L. Chen, X. G. Chen, Determination of pathogenic bacteria–*Bacillus anthrax* spores in environmental samples by ratiometric fluorescence and test paper based on dual-emission fluorescent silicon nanoparticles, *J. Hazard. Mater.* 2020, **386**, 121956.
 11. K. Luan, R. Q. Meng, C. F. Shan, J. Cao, J. G. Jia, W. S. Liu, Y. Tang, Terbium functionalized micelle nanoprobe for ratiometric fluorescence detection of anthrax spore biomarker, *Anal. Chem.* 2018, **90**, 3600–3607.
 12. X.Q. Li, J.J. Luo, L. Deng, F.H. Ma, M.H. Yang, In situ incorporation of fluorophores in zeolitic imidazolate framework-8 (ZIF-8) for ratio-dependent

- detecting a biomarker of anthrax spores, *Anal. Chem.* 2020, **92** 7114–7122.
13. M. C. Rong, X. Z. Deng, S. T. Chi, L. Z. Huang, Y. B. Zhou, Y. N. Shen, X. Chen, Ratiometric fluorometric determination of the anthrax biomarker 2,6-dipicolinic acid by using europium (III)-doped carbon dots in a test stripe, *Mikrochim Acta* 2018, **185**, 201.
14. S. M. Qu, N. Z. Song, G. X. Xu, Q. Jia, A ratiometric fluorescent probe for sensitive detection of anthrax biomarker based on terbium-covalent organic polymer systems, *Sens, Actuators B Chem.* 2019, **290**, 9–14.
15. Q. J. Zhou, Y. J. Fang, J. Y. Li, D. Hong, P. P. Zhu, S. H. Chen, K. J. Tan, A design strategy of dual-ratiometric optical probe based on europium-doped carbon dots for colorimetric and fluorescent visual detection of anthrax biomarker, *Talanta*, 2021, **222**, 121548.